

# Informative Scene Graph Generation via Debiasing

Lianli Gao<sup>1</sup>, Xinyu Lyu<sup>1</sup>, Yuyu Guo<sup>1</sup>, Yuxuan Hu<sup>2</sup>, Yuan-Fang Li<sup>3</sup>, Lu Xu<sup>4</sup>, Heng Tao Shen ACM/IEEE Fellow<sup>1</sup> and Jingkuan Song<sup>1\*</sup>

<sup>1</sup>Center for Future Media & School of Computer Science and Engineering, University of Electronic Science and Technology of China, Chengdu, Sichuan, China.

<sup>2</sup>Southwest University, Chongqing, China.

<sup>3</sup>Monash University, Melbourne, Victoria, Australia.

<sup>4</sup>Kuaishou, Beijing, China.

\*Corresponding author(s). E-mail(s): [jingkuan.song@gmail.com](mailto:jingkuan.song@gmail.com);

## Abstract

Scene graph generation aims to detect visual relationship triplets, (subject, predicate, object). Due to biases in data, current models tend to predict common predicates, *e.g.*, “on” and “at”, instead of informative ones, *e.g.*, “standing on” and “looking at”. This tendency results in the loss of precise information and overall performance. If a model only uses “stone on road” rather than “stone blocking road” to describe an image, it may be a grave misunderstanding. We argue that this phenomenon is caused by two imbalances: semantic space level imbalance and training sample level imbalance. For this problem, we propose DB-SGG, an effective framework based on debiasing but not the conventional distribution fitting. It integrates two components: Semantic Debiasing (SD) and Balanced Predicate Learning (BPL), for these imbalances. SD utilizes a confusion matrix and a bipartite graph to construct predicate relationships. BPL adopts a random undersampling strategy and an ambiguity removing strategy to focus on informative predicates. Benefiting from the model-agnostic process, our method can be easily applied to SGG models and outperforms Transformer by **136.3%**, **119.5%**, and **122.6%** on mR@20 at three SGG sub-tasks on the SGG-VG dataset. Our method is further verified on another complex SGG dataset (SGG-GQA) and two downstream tasks (sentence-to-graph retrieval and image captioning).

**Keywords:** Scene Graph Generation, Visual Relationship, Debiasing, Information Content.

## 1 Introduction

Scene Graph Generation (SGG) aims to detect instances and their visual relationships in an image. It provides a structured vision representation, as an auxiliary tool, to bridge the gap between computer vision and natural language, supporting many high-level tasks such as image captioning (Anderson et al., 2018; Yao, Pan, Li, Qiu, & Mei, 2017; M. Zhang et al., 2019), visual

question answering (W. Guo, Zhang, Yang, & Yuan, 2021; X. Li et al., 2019; Teney, Liu, & van den Hengel, 2017; L. Zhao, Lyu, Song, & Gao, 2021) and visual retrieval (Johnson et al., 2015; Schuster, Krishna, Chang, Fei-Fei, & Manning, 2015; Shen et al., 2016; Song et al., 2018; Zeng, Gao, Lyu, Jing, & Song, 2021).

Inspired by remarkable progress in object detection (Girshick, 2015; Girshick, Donahue,

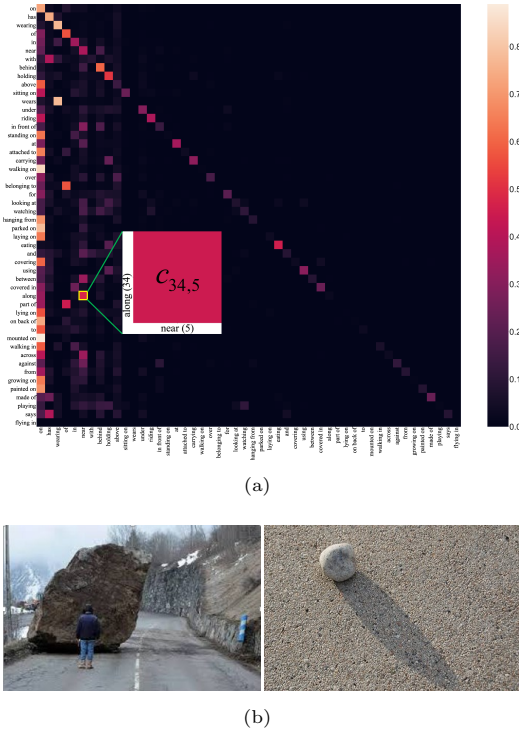


**Fig. 1** (a) A confusion matrix of a baseline model. The element  $c_{i,j}$  represents the number of samples labeled as predicate category  $i$  but predicted as  $j$ . The results of the model concentrate on the more common predicates (towards the left of the confusion matrix) such as “on” and “near”. (b) Two search results for “stone on road” in Google. If the model directly uses the common predicate “on” to describe the first image like the second image in (b), it may cause serious consequences.

Darrell, & Malik, 2016; Redmon, Divvala, Girshick, & Farhadi, 2016), existing solutions (Herzig, Raboh, Chechik, Berant, & Globerson, 2018; Y. Li et al., 2018; Xu, Zhu, Choy, & Fei-Fei, 2017; Yin et al., 2018) mostly follow a common generation pipeline, that is, firstly detecting instances from an image, extracting region features of instances, and then classifying the predicate categories under the guidance of a standard classification objective function. Due to biases in data, current state-of-the-art methods, however, exhibit the tendency that most of the recognized predicates are general or common (e.g., “on” or “in”) but not specific or informative ones (e.g., “standing on” or “sitting on”), as shown in Fig. 1(a). Thus, it is hard to apply an SGG model in the real world, since the generated scene graphs provide insufficient clues and may lead to misunderstanding of a scene. In this work, our study reveals that such biased

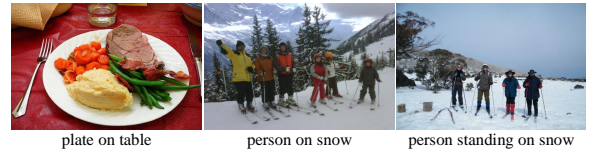


**Fig. 2** Ground-truth annotations from the Visual Genome dataset. The first and second examples are marked as “on” because of the huge semantic space of “on”. Compared with “person standing on snow” in the third example, “person on snow” in the second example is ambiguous and information-poor.

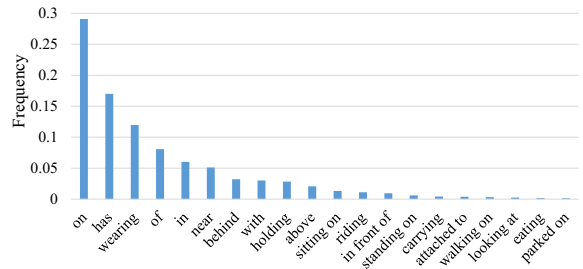


**Fig. 3** Frequencies of some predicates in the Visual Genome dataset. For clarity, we omit some predicates.

predicates are caused by the imbalance issue, which substantially limits the performance of well-designed SGG models. Specifically, this issue can be further divided into two key problems: *semantic space level imbalance* and *training sample level imbalance*.

**Semantic space level imbalance.** Common predicates such as “on” have large semantic spaces, while more informative predicates like “standing on” provide richer content but have small semantic spaces. They may even be replaced by more common ones in some annotations. An example of this semantic space level imbalance is shown in Fig. 2, in which all examples reflect the fact of “on”, while only the last two examples represent the more specific information of “standing on”. Although “standing on” is more precise for the second image, it may still be annotated by humans annotators with “on” because of its larger semantic space than “standing on”. Tagging different labels for identical contents confuses the SGG model and causes poor performance.

**Training sample level imbalance.** When learning to recognize predicates, samples of informative predicates are particularly valuable as they provide precise knowledge to a scene graph. However, samples are dominated by the common predicate categories in SGG datasets such as Visual

Genome (SGG-VG) (Krishna et al., 2017), as discussed in previous works (Tang, Niu, Huang, Shi, & Zhang, 2020; Yu, Chai, Wang, Hu, & Wu, 2021). For example, Fig. 3 shows the sample distribution over predicate categories of SGG-VG. We can observe that the number of common predicate samples is much larger than that of informative ones, which leads to the problem of the long-tailed distribution of the classes. Within such an imbalanced sampling space, the prediction of informative predicates is dominated by the common ones.

The above challenges motivate us to study two problems: 1) how to revise common predicates as informative ones based on their semantic relationship, and 2) how to make the sample space balanced for training. To tackle these problems, we believe that the key is to explore the predicate relationships in the semantic space and adjust the sampling space to be balanced. Motivated by this, we propose a simple yet effective pipeline, namely, *Scene Graph Generation via Debiasing* (DB-SGG), to generate informative scene graphs. This pipeline integrates two novel components: 1) Semantic Debiasing (SD), which improves informative predictions with rich information contents by fully exploiting semantic relationships among predicates, and 2) Balanced Predicate Learning (BPL), which focuses on informative predicates according to their information contents.

How to estimate semantic relationships among predicates in Semantic Debiasing (SD)? We find that the confusion matrix of a baseline model can estimate the predicate relationships to a certain extent, as shown in Fig. 1(a). Therefore, this matrix is utilized in SD firstly. However, constructing the confusion matrix requires the ground truth annotations and evaluation of the model on the dataset. To save the process of constructing the confusion matrix, we design another automatic method that only uses subject-object labels involved in predicates to build a bipartite graph of the predicate relationship. Balanced Predicate Learning (BPL) needs the model to focus on informative predicates. Consequently, an adjusted domain dominated by informative predicates is designed by undersampling common predicates. We firstly adopt a random undersampling strategy for common predicates to improve the informativeness of the adjusted domain. Moreover,

tagging different labels for identical contents produces ambiguous samples and confuses the SGG model, as shown in Fig. 2. We, therefore, propose an ambiguity removing strategy to eliminate the impact of ambiguous samples.

In summary, the main contributions of our work are fourfold:

- We systematically review the process of scene graph generation and reveal the problem of insufficient information contents that limit SGG’s overall performance and practical applicability. We delineate this problem as *semantic space level imbalance* and *training sample level imbalance*.
  - We propose DB-SGG for informative scene graph generation, a novel framework that adjusts biased predicate predictions by two components: semantic debiasing (SD) and balanced predicate learning (BPL). It is worth noting that DB-SGG, with its model-agnostic components, can be easily plugged into existing models.
  - Evaluated on Visual Genome (SGG-VG), our proposed DB-SGG framework obtains significant improvements over state-of-the-art SGG approaches. Our method improves Transformer by 136.3%, 119.5%, and 122.6% on Mean Recall@20 in the three scene graph generation sub-tasks respectively.
  - We introduce predicate information content to reflect the overall trend of informativeness. Based on predicate information content, we propose a new metric (mRIC@K) that provides a general and straightforward measure of the informativeness of the generated scene graph.
- This paper is extended from our conference version (Y. Guo et al., 2021). The new contributions are summarized as follows:
- For the semantic debiasing (SD) module, we propose a bipartite graph structure based on subject-object label overlap to construct the semantic relationship among predicates, which save the process of constructing the confusion matrix.
  - For balanced predicate learning (BPL), we further elaborate an ambiguity removing strategy and combine it with the bipartite graph structure to eliminate the impact of ambiguous samples.

- We conduct experiments on another complex dataset, *i.e.*, SGG-GQA (Hudson & Manning, 2019). Compared with SGG-VG, SGG-GQA contains more object categories (1704) and predicate categories (311) with a complex environment.
- We adopt two downstream tasks (sentence-to-graph retrieval and image captioning) to verify the practicability and informativeness of generated scene graphs.

## 2 Related Work

### 2.1 Scene Graph Generation

Many methods (M. Chen et al., 2022; Y. Li et al., 2018; Lyu, Gao, Guo, et al., 2022; Lyu, Gao, et al., 2023; Lyu, Gao, Zeng, Shen, & Song, 2022; Lyu, Liu, Guo, & Gao, 2023; S. Wang et al., 2022; Xu et al., 2017; Yin et al., 2018; Zhan, Yu, Yu, & Tao, 2020; Zheng, Gao, et al., 2023; Zheng, Lyu, Gao, Dai, & Song, 2023; Zheng et al., 2022) have been proposed to handle the scene graph generation task in recent years. These methods tackle the task from different perspectives. Some extract context information by message passing (X. Lin, Ding, Zeng, & Tao, 2020; Mi & Chen, 2020; Xu et al., 2017; Zellers, Yatskar, Thomson, & Choi, 2018). Some construct visual embeddings in the semantic space (Hung, Mallya, & Lazebnik, 2020; Newell & Deng, 2017; H. Zhang, Kyaw, Chang, & Chua, 2017). Some propose to improve model’s robustness by utilizing external knowledge (Gu et al., 2019; Y. Guo, Song, Gao, & Shen, 2020; Kan, Cui, & Yang, 2021, 2022; Lu, Krishna, Bernstein, & Li, 2016). Some explore efficient end-to-end structures to improve model’s inference efficiency (R. Li, Zhang, & He, 2022; Liu, Yan, Mortazavi, & Bhanu, 2021).

In experiments, we choose three representative and state-of-the-art models as our baselines: MotifNet (Zellers et al., 2018), VCTree (Tang, Zhang, Wu, Luo, & Liu, 2019) and Transformer (Vaswani et al., 2017), all of which have been implemented in the Scene Graph Generation Benchmark (Tang, 2020). We discuss these models in detail below.

**MotifNet:** Zellers et al. (Zellers et al., 2018) explored regularly appearing substructures, namely motifs, in scene graphs. In order to capture the high-level motifs, they introduced MotifNet

to encode the global context. MotifNet divides the process of scene graph generation into two steps: an object context encoder and an edge context encoder. The object context encoder refines object labels and captures the object context. The edge context encoder is designed to predict the relationship predicates of each object pair. Both the object encoder and the edge encoder use Bi-LSTMs for capturing the global context.

**VCTree:** Tang et al. (Tang et al., 2019) placed the instances of an image into a dynamic tree structure and captured the hierarchical contextual information. Compared with the fixed chain structure and dense graph, the proposed dynamic tree adaptively adjusts the structure and captures hierarchical information according to the content. They integrate supervised learning and reinforcement learning for exploring the dynamic tree structure in the image.

**Transformer:** The Transformer (Tang, 2020) structure based on the self-attention mechanism has been utilized to handle problems in natural language and computer vision. Specifically, it replaces the Bi-LSTMs with Transformer Encoders in entity/edge context encoder of the MotifNet. We note that Transformer has also been employed in a number of other recent SGG methods (Y. Guo et al., 2020; X. Lin et al., 2020; Lyu, Gao, Guo, et al., 2022; Lyu, Gao, Zeng, et al., 2022; Tang et al., 2020).

However, due to the bias in the dataset, the results of most previous methods are also biased. To relieve this problem, Y. Liang et al. (2019) reconstructed a dataset that focuses on visually-relevant relationships for learning an unbiased model. Another unbiased SGG method (Tang et al., 2020) attempted to remove the vision-agnostic bias with counterfactual causality. The cognition tree structure is proposed by Yu et al. (2021) to balance the loss of the model. EBM (Suhail et al., 2021) considers the structural information in the output space for semantic debiasing. BGNN (R. Li, Zhang, Wan, & He, 2021) employs up-sampling strategies for balanced learning process.

Different from these works, our analysis on why previous models focus on predicting common predicates reveals two types of imbalances, namely semantic space level imbalance and training sample level imbalance. In view of the two imbalances,

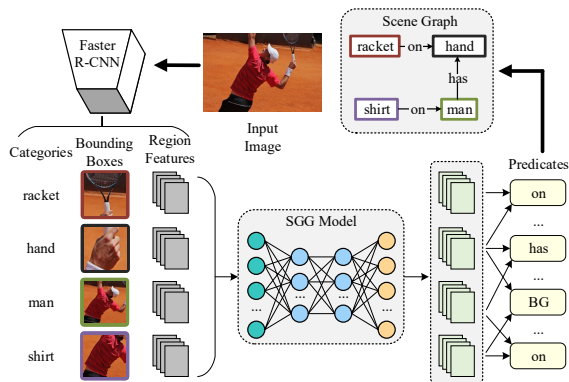


**Fig. 4** The main process of previous methods that maps an input image to its scene graph.

our method explores the imbalance in the semantic and learning space effectively to learn scene graphs with precise and rich information. Moreover, we define the informativeness of predicates by the information content, which provides a general way to explore the value of generated scene graphs.

## 2.2 Informative Prediction

Many works have been proposed to avoid only predicting common object categories or common words in computer vision tasks such as fine-grained recognition (Y. Chen, Bai, Zhang, & Mei, 2019; Lam, Mahasseni, & Todorovic, 2017; Y. Wang, Morariu, & Davis, 2018) and informative image captioning (Cohn-Gordon, Goodman, & Potts, 2018; S. Zhao, Sharma, Levinboim, & Soricut, 2019). Most of them focus on the informative object categories, which are either precisely represented by samples or constructed with distinct hierarchies. Unlike object categories, it is difficult to define a clear hierarchical or coarse-to-fine structure for relationship predicates in scene graph generation. Another general way to measure informativeness is information content (McMahon, 2007; Ross, 2014), which is the negative log probability and reflects how *surprising* an event is. When a rare event occurs, it is more surprising and contains more information than common events. Previous works (D. Lin, 1998; Pedersen, 2010; Resnik, 1995) utilized this definition to measure the informativeness of concepts in natural language processing. In scene graph generation, similarly, the relationship predicates can also be extracted from natural language and can

be described by their information content. Therefore, we use this definition to distinguish common and informative predicates.

## 3 Approach

### 3.1 Approach Overview

**Problem Formulation.** As shown in Fig. 4, conventional methods formulate scene graph generation as a two-stage process, where it firstly detects all instances-of-interest and then recognizes relationship predicates between pair-wise instances. Given an image  $\mathbf{X}$ , its corresponding scene graph is generated from the complete graph  $\mathbf{G} = \langle \mathbf{O}, \mathbf{R} \rangle$ , where  $\mathbf{O} = \{o_i\}$  are instance nodes.  $\mathbf{R} = \{r_i\}$  is the full set of edges, each of which connects two nodes and encodes a relationship between them. More specifically, each edge is represented in the form of a triplet  $(o_i, y_{ij}, o_j)$ , where  $o_i$  denotes the subject,  $o_j$  is the object, and  $y_{ij}$  represents the predicate of the edge/triplet. We denote by  $\mathbf{Y}$  the list of predicate labels for the edges  $\mathbf{R}$ , hence  $|\mathbf{Y}| = |\mathbf{R}| = |\mathbf{O} \times \mathbf{O}|$ , where  $|\cdot|$  represents the length/size of a list/set.

The pair of  $(o_i, o_j)$  is embodied as region bounding boxes with object categories, which are usually obtained by an object detector such as Faster R-CNN (Ren, He, Girshick, & Sun, 2017). Thus, SGG models omit the process of object detection and only focus on predicting relationship predicates  $\mathbf{Y}$  between instance pairs, by maximizing the probability  $\Pr(\mathbf{Y} | \mathbf{O} \times \mathbf{O}; \theta)$ , where  $\theta$  is the learnable parameter of the scene graph generation model.

**Overview.** We follow this pipeline approach and focus on the second stage, *i.e.*, predicate recognition, after instance regions are detected by an object detection system. In particular, the proposed method consists of two processes, as shown in Fig. 5. 1) Semantic Debiasing (SD) is applied to improve informative prediction from a biased model, where it performs a relation modeling among predicates. 2) Balanced Predicate Learning (BPL) is designed for extending the sampling space for informative predicates. In the following subsections, we present details of each component.

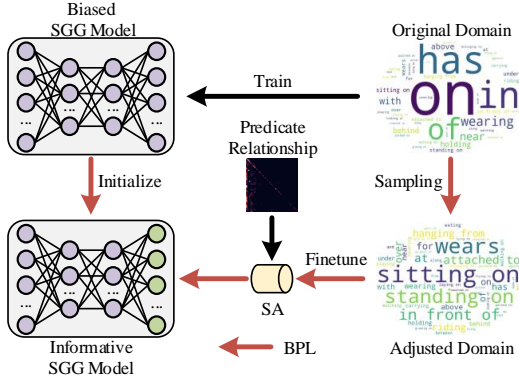


**Fig. 5** The overall training process of our method, including Semantic Debiasing (SD) and Balanced Predicate Learning (BPL).

### 3.2 Semantic Debiasing (SD)

As we discussed earlier, most of the current SGG models bias toward the common predicate classes. The Semantic Debiasing component is designed to restore informative predictions from common ones predicted by a biased model, based on the semantic relationship between predicates. Intuitively, “standing on” is more likely to be predicted as “on” than “has” because the meanings of “standing on” and “on” are closer than between “standing on” and “has”. Therefore, we exploit such relationships to adjust the prediction of a biased SGG model. In particular, we formalize this debiasing as Equation (1):

$$\Pr(\mathbf{Y} | \mathbf{O} \times \mathbf{O}; \theta) = \prod_{o_i, o_j \in \mathbf{O}} \Pr(y_{ij}^s | o_i, o_j; \theta),$$

$$\Pr(y_{ij}^s | o_i, o_j; \theta) = \Pr(y_{ij}^s | y_{ij}^g) \Pr(y_{ij}^g | o_i, o_j; \theta), \quad (1)$$

where  $\Pr(y_{ij}^g | o_i, o_j; \theta) \in \mathbb{R}^K$  is the prediction of the biased SGG model for all predicate categories between subject  $o_i$  and object  $o_j$ ,  $\Pr(y_{ij}^s | o_i, o_j; \theta) \in \mathbb{R}^K$  is produced by the SGG model after semantic debiasing, and  $K$  is the total number of predicate categories.  $\Pr(y_{ij}^s | y_{ij}^g)$  represents the semantic debiasing, which measures how confident a common result is transformed into an informative one.

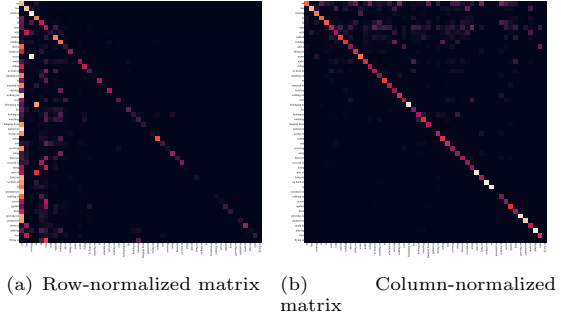


**Fig. 6** Confusion matrices using different normalization strategies.

Specifically, the prediction  $\Pr(y_{ij}^s | o_i, o_j; \theta)$  can be factorized as follows:

$$\Pr(y_{ij}^s = l | o_i, o_j; \theta) = \sum_{h=1}^K \underbrace{\Pr(y_{ij}^s = l | y_{ij}^g = h)}_{\text{semantic debiasing}} \underbrace{\Pr(y_{ij}^g = h | o_i, o_j; \theta)}_{\text{biased model}}. \quad (2)$$

Thus, the prediction of the informative model producing label  $l$  between subject  $o_i$  and object  $o_j$  is the sum of the product of the semantic debiasing and the biased model producing label  $h$ .

The semantic debiasing  $\Pr(y_{ij}^s | y_{ij}^g)$  reflects the latent semantic relationship between predicates. It can be considered as a transition matrix between pairs of predicate labels, thus is of dimension  $K \times K$ . In this section, we introduce two methods, *i.e.*, confusion matrix and bipartite graph, to construct this transition matrix.

#### 3.2.1 Semantic Debiasing with Confusion Matrix (SDCM)

For simplicity, we denote  $\Pr(y_{ij}^s | y_{ij}^g)$  as a transition matrix  $C^* \in \mathbb{R}^{K \times K}$ , and it can be derived from prediction priors. We denote by  $C \in \mathbb{R}^{K \times K}$  the prediction confusion matrix, where each element  $c_{kl}$  denotes the number of samples labeled as the  $k$ -th category but being predicted as  $l$ . In this paper, we use the frequency model (Zellers et al., 2018) to generate predictions on the training dataset for  $C$ , and fix it in our framework. Next, a normalized transition matrix  $C'$ , in which each

element  $c'_{kl}$  is defined in Equation (3) as follows:

$$c'_{kl} = \frac{c_{kl}}{\sum_{m=1}^K c_{km}} . \quad (3)$$

The visualization of the row-normalized confusion matrix is shown in the heatmap in Fig. 6(a). We can observe that large values of the matrix concentrate on the left side. This implies that many informative predicates are classified as a few common ones. The matrix also implies the semantic relationship between predicates to some extent, *e.g.*, “parked on” is more likely to be predicted “on” than “has”. It can also be observed that the non-diagonal highlighted elements in the row-normalized confusion matrix are brighter than the column-normalized matrix, as shown in Fig. 6(b). Thus, predicate relationships are more evident in the row-normalized matrix, and the row-normalized matrix can better represent the relationship among predicates than the column-normalized one. Therefore, we use the row-normalized matrix to transform prediction instead of the transpose of the column-normalized matrix. However, if an informative predicate has been predicted, its prediction should not be adjusted significantly. Directly multiplying  $C'$  may greatly decrease the score of an informative predicate because the diagonal tail values are small. Therefore, the diagonal elements’ values should be increased to alleviate this impact. To achieve this goal, we add a weighted identity matrix to  $C'$ , resulting in the final transition matrix  $C^*$  as formed by Equation (4):

$$C^* = \text{Row\_Normalize}(C' + \alpha I_K) , \quad (4)$$

where  $I_K \in \mathbb{R}^{K \times K}$  is the identity matrix.  $\alpha$  is a hyper-parameter to adjust the importance of the identity matrix. Normalizing the matrix by row ensures that the sum of the row is 1. We freeze the transition matrix during training to avoid semantic drifting. Semantic Debiasing with Confusion Matrix is denoted as SDCM.

### 3.2.2 Semantic Debiasing with Bipartite Graph (SDBG)

In addition to the confusion matrix, we also introduce a model-free method to find the semantic relationship between predicates. We design

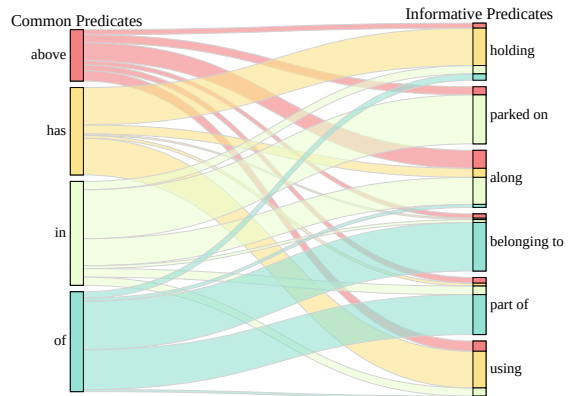


**Fig. 7** A bipartite graph constructed by the subject-object overlap in Visual Genome. We choose a sub-graph from the whole bipartite graph for clarity. The thicker the line, the stronger the relation.

a bipartite graph to improve informative predictions. In natural language, the subject-object pairs involved in a predicate greatly reflect the semantics of the predicate. For example, both “walking on” and “standing on” involve many subject-object pairs, such as “man-snow” and “man-street”. Therefore “walking on” and “standing on” have similar semantics. Inspired by this intuition, we use the subject-object label overlap between predicates to define the predicate relationship.

We first define the semantic representation  $S_k \in \mathbb{N}^{V \times V}$  ( $V$  is the total number of instance categories) of the predicate  $k$  with involved subject-object labels  $m$  and  $n$  as follows:

$$s_{kmn} = \begin{cases} 1, & \text{if } \langle k, m, n \rangle \text{ in training set} \\ 0, & \text{otherwise} \end{cases} , \quad (5)$$

where  $\langle k, m, n \rangle$  represents the triplet label “predicate label, subject label, object label”. Then the semantic relation between the predicate  $k$  and the predicate  $l$  can be computed as follows:

$$\tilde{c}_{kl} = \sum_{m=1}^V \sum_{n=1}^V s_{kmn} \times s_{lmn} . \quad (6)$$

Since the semantic debiasing needs to restore informative predicates from common ones, we design a directed bipartite graph  $\tilde{C} \in \mathbb{R}^{K \times K}$

between the common predicates and the informative predicates to construct the transition matrix:

$$\tilde{c}_{kl} = \begin{cases} \tilde{c}_{kl} & \text{if } k \text{ informative, } l \text{ common} \\ 0 & \text{otherwise} \end{cases} . \quad (7)$$

The definitions of common and informative predicates will be introduced in Sect. 3.3. Similarly, we use Equation (4) to normalize the bipartite graph and construct  $\Pr(y_{ij}^s | y_{ij}^g)$ . A bipartite graph of some common predicates and informative predicates is shown in Fig. 7. We can observe that the relationship between “belonging to” and “of” is stronger than that between “belonging to” and “in”. In natural language, the meaning of “belonging to” is more similar to “of” than “in”. Therefore, the subject-object overlap can effectively represent the semantic relationship between predicates. We denote Semantic Debiasing with Bipartite Graph as SDBG.

Besides the empirical intuition as mentioned above, the dataset with rich annotations is also the basis of our method. Since the SGG dataset is annotated by humans and contains abundant annotations and samples, prior knowledge in the dataset well reflects human’s real reflection of the visual world. Therefore, we construct the confusion matrix/bipartite graph from the SGG dataset.

### 3.3 Balanced Predicate Learning (BPL)

To address the problem of imbalanced training, a new adjusted data source with a balanced sample space is needed. Formally, we view a data source with an imbalanced sample space as an original domain (*i.e.*, the original dataset), and a data source with a relatively balanced sample space as an adjusted domain. Unlike existing methods that train the SGG model in the original domain only, Balanced Predicate Learning (BPL) divides the learning process into three stages: 1) training an SGG model on an original domain; 2) creating an adjusted domain; and 3) transfer learning on the adjusted domain. Fig. 5 shows the overview of this learning process.

**Resample:** In the first stage, we take a common training strategy that is identical to that of previous works (Xu et al., 2017; Zellers et al., 2018) to train an SGG model on the original domain.

In the second stage, an adjusted domain with a relatively balanced sample space is constructed. However, it is hard to decide whether a predicate is informative or not as no such annotations are available. Intuitively, common predicates are semantically more general, while informative predicates are more specific. Therefore, the above discriminative problem can be transformed into a measurement that measures how informative a predicate is. In other words, how much information content does a predicate involves. According to Shannon’s information theory, the information content  $I$  of an event  $z$  (*i.e.*, predicate) can be measured by Equation (8):

$$I(z) = -\log_b[\Pr(z)] , \quad (8)$$

where  $\Pr(z)$  denotes the probability of the event  $z$ . It reflects the fact that an event with a small probability provides more information content. Inspired by this, we measure informativeness for each predicate category by estimating its information content, using Equation (8). The probability of a predicate category is estimated by its frequency in datasets. Then, its information content is weighted by the negative-log probability with base (b). An example of this is shown in Fig. 3, where predicate “on” has a higher occurrence frequency hence a lower information content when compared with “standing on”. Besides our work, frequency-based information content is widely used in semantic similarity measures (Resnik, 1995, 1999; Seco, Veale, & Hayes, 2004) and information retrieval (Robertson, 2004). It is noteworthy that other ways of calculating ‘informativeness’, *e.g.*, semantic context based method (C. Liang, Wu, Huang, & Giles, 2015) or statistical information in corpora by TF-IDF (Salton & Buckley, 1988), can also be used here. We calculate ‘informativeness’ based on Shannon information theory mainly for simplicity and generality. Instead of explaining all examples perfectly, the definition reflects the overall trend of information content, *i.e.*, on the whole, tail predicates usually have more information than head predicates.

Based on a specific information source (*e.g.*, Visual Genome and Wikipedia), the frequency for each predicate category is used to calculate its information content. We sort all predicates by their information content.  $M$  predicates with the



least information contents are chosen as common ones and the rest are informative predicates. Next, we create an adjusted domain by sampling labeled data from the original domain in two ways.

### 3.3.1 Balanced Predicate Learning with Random Undersampling (BLRU)

A direct way is a balanced sampling strategy that increases the sampling frequency of rare categories. However, such an upsampling strategy is ineffective for the scene graph generation task, as demonstrated in previous work (Tang et al., 2020). Therefore, we take a separation undersampling strategy to create an adjusted domain. In particular, we move all samples that belong to the informative predicate categories in the original domain to the adjusted domain. As for categories belonging to the  $M$  common predicates, we randomly sample  $N$  labeled triplet samples from the original domain for each predicate, resulting in a more balanced sample space between common predicates. Practically, it is made by randomly discarding ground-truth annotations per image for those “common” predicates until their amounts decrease to  $N$ . Thus, it produces an adjusted domain containing  $M * N$  “common” predicates and all the “informative” ones. Practically,  $N$  would be smaller than the minimum of available triplet samples from those  $M$  predicates. Besides balancing the dataset, randomly removing samples of common predicates may also produce another benefit: as there are many ambiguous samples for common predicates that may interfere with informative predicates, as shown in Fig. 2, reducing samples of common predicates may help to reduce the impact of these samples to a certain extent. The Balanced Predicate Learning with Random Undersampling is denoted as BLRU.

### 3.3.2 Balanced Predicate Learning with Removing Ambiguous Samples (BLRA)

We also introduce an empirical undersampling method to eliminate the impact of ambiguous samples mentioned in Sect. 1, *i.e.*, identical contents tagged with different predicate labels. The first problem is how to define or select ambiguous

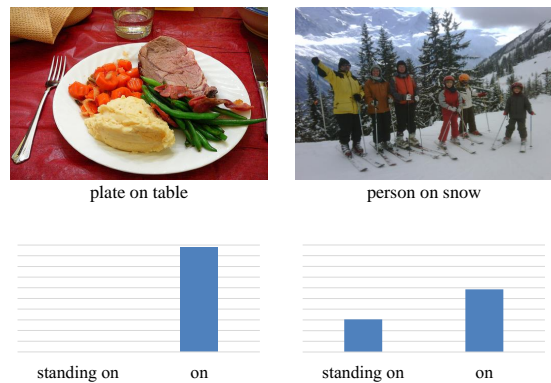


**Fig. 8** Ground-truth annotations in the top and prediction scores in the bottom from Visual Genome. The first and second examples are both annotated as “on”. Compared with the first example, the second example is ambiguous and can be annotated as either “on” or “standing on”. The bar graphs show scores predicted by the model pre-trained in the original domain for each example. We only show the scores of “on” and “standing on” for clarity.

samples. As shown in Fig. 8, the second example is ambiguous because it can be annotated as either “on” or “standing on”. Compared with the first example, which can only be labeled as “on”, labeling the second sample as “on” has lower confidence. However, it is too expensive to set the confidence of samples manually. In this paper, we use an SGG model pre-trained in the original domain to find ambiguous samples in common predicates by their confidence and remove them in the adjusted domain. More specifically, we remove triplet examples with low scores in common predicates and keep the top- $N$  highest triplet examples for each common predicate in the adjusted domain. The Balanced Predicate Learning with Removing Ambiguous Sample is denoted as BLRA.

After adjusted domain construction, we can finally train an informative SGG model on it. Instead of training the model from scratch on the adjusted domain, we first initialize an SGG model from the one pre-trained in the first stage. Then, only the last recognition layer of the SGG model is finetuned on the adjusted domain. There are two reasons behind this: First, finetuning the whole model incurs high computation costs. Second, training the whole model on the adjusted domain with fewer labeled samples increases the risks of overfitting, leading to an unreliable model. More details can be seen in Sect. 4.5. Although our

method requires more training steps, it is comparable to the previous models in the inference stage since our method does not significantly change the model structures.

## 4 Experiments

In this section, we first describe experimental settings, including metrics, datasets and implementation details. Then, we perform an empirical evaluation to demonstrate the superiority of our method. Lastly, we conduct ablative studies on the proposed components and provide more insights with qualitative and quantitative analyses.

### 4.1 Metrics

**Scene Graph Generation.** Following previous works (T. Chen, Yu, Chen, & Lin, 2019; Tang et al., 2020, 2019), we evaluate the SGG method on three subtasks: 1) Predicate Classification (PredCls), 2) Scene Graph Classification (SGCls), and 3) Scene Graph Detection (SGDet). The PredCls task takes ground truth bounding boxes and labels as inputs. The SGCls task takes ground truth object bounding boxes as inputs, but without labels. The SGDet task requires the prediction of relationships from scratch.

In this work, we use three evaluation metrics: R@K, mR@K and mRIC@K. R@K averages the recall across all samples, while mR@K calculates R@K for each predicate category and averages the recall across all predicate categories. For an imbalanced dataset like Visual Genome, R@K focuses on common predicates with rich samples and underestimates informative predicate categories. Due to the biased nature of R@K, we report our main evaluation results with the mR@K metric following previous works (T. Chen et al., 2019; Tang et al., 2020, 2019; Yu et al., 2021).

Moreover, we propose a new metric, mRIC@K, that measures the mean recall with information content. Specifically, for each predicate, its recall with information content, denoted RIC, is calculated by multiplying its recall with the predicate’s information content, which is calculated by Equation (8) with  $b$  as 2. mRIC@K, finally, can be obtained by averaging the RIC values across all predicate categories. This metric reflects how much information a scene graph can provide. A higher score implies that the generated

scene graph involves more informative content and vice versa. Moreover, we use two information sources to estimate information content for each predicate, *i.e.*, Visual Genome and Wikipedia. For Wikipedia, we find all predicate categories of Visual Genome in the Wikipedia corpus by word matching and count their frequencies as their probabilities. Then, the information content from Wikipedia is calculated by Equation (8) for each predicate category. For simplicity, we separately denote by mRIC (VG) and mRIC (Wiki) the respective information content computed from Visual Genome and Wikipedia.

**Sentence-to-Graph Retrieval.** To verify the effectiveness of generated scene graphs, we use sentence-to-graph retrieval as a downstream task following Tang et al. (2020). In this task, the SGG method extracts scene graphs from images without any ground truths (*i.e.*, SGDet) firstly. Extracted scene graphs and image captions are then embedded in a joint space. In the test phase, the scene graph embeddings are queried by the image caption embeddings on a gallery. The recall@20/50/100 are reported on the  $1k/5k$  gallery in our experiments.

**Image Captioning.** Besides the sentence-to-graph retrieval, the image captioning task is also utilized to verify the informativeness of scene graphs. In this task, we combine object visual features and scene graphs to generate image captions. The metrics include Bleu (Papineni, Roukos, Ward, & Zhu, 2002), Meteor (Denkowski & Lavie, 2014), Cider (Vedantam, Zitnick, & Parikh, 2015), and Spice (Anderson, Fernando, Johnson, & Gould, 2016), which are standard evaluation methods for image captioning.

### 4.2 Datasets

**Scene Graph Generation.** Following previous works (T. Chen et al., 2019; Tang et al., 2020; Zellers et al., 2018), we conduct experiments on a widely used SGG dataset, namely Visual Genome (SGG-VG). It is composed of 108k images across 75k object categories together with 37k predicate classes. Since 92% of the predicates have few samples, following many previous works (L. Chen et al., 2019; T. Chen et al., 2019; Xu et al., 2017; Yu et al., 2021; Zellers et al., 2018), we adopted the widely-used VG split, where it contains the

most frequent 150 object categories and 50 predicate classes. Moreover, the VG dataset is split into a training set (70%) and a test set (30%), and we further sample a validation set (5k) from the training set for model validation. The experimental results are reported in the SGG-VG dataset unless otherwise specified.

Besides the Visual Genome split (Zellers et al., 2018), we also use another SGG dataset from Question Answering on Image Scene Graphs (GQA) (Hudson & Manning, 2019), namely SGG-GQA, to verify our method. This dataset is also collected from Visual Genome but contains denser annotations (1704 object classes and 311 predicate classes). In total, there are about 75k images in the training set and 10k images in the testing set. We further sample a validation set (5k) from the training set.

**Sentence-to-Graph Retrieval.** For the sentence to graph retrieval task, we follow the setting of Tang et al. (2020), which contains about 41k images from Visual Genome and MS-COCO (T. Lin et al., 2014), and split 1k/5k images in the test set.

**Image Captioning.** For the image captioning task, we follow the setting of Vedantam, Bengio, Murphy, Parikh, and Chechik (2017), which contains about 113k images in the training set, 5k images in the validation set and 5k images in the test set from MS-COCO (T. Lin et al., 2014).

### 4.3 Implementation Details

**Scene Graph Generation.** Our framework is designed to be easily pluggable into existing SGG methods to improve their performance, especially on more informative predicates. In this work, we evaluate our method’s performance on three strong baselines: **MotifNet** (Zellers et al., 2018), **VCTree** (Tang et al., 2019) and **Transformer** (Tang, 2020; Vaswani et al., 2017). The numbers of inner layers in the object encoder and the edge encoder are set to 4 and 2, respectively. Other hyperparameters are also identical to the setting in **Model Zoo** (Tang, 2020). All models share the same Faster R-CNN pre-trained on Visual Genome.

We utilize Faster R-CNN (Ren et al., 2017) with ResNeXt-101-FPN (He, Zhang, Ren, & Sun, 2016; T. Lin et al., 2017; Xie, Girshick, Dollár, Tu, & He, 2017) pre-trained by Tang et al. (2020) to

detect instances in images and freeze the weights during learning of scene graph generation. For scene graph generation, we firstly train all SGG models on the original domain according to the recommended configuration (Tang, 2020) for all tasks, including the learning rate and batch size. Each model is then finetuned on the adjusted domain with the same configuration. We take the logits before the softmax layer as  $\Pr(y_{ij}^g | o_i, o_j; \theta)$  in Equation (1) for the sake of simplicity. For constructing the adjusted domain,  $M$  predicates with the smallest information content are set as common predicates, where  $M$  is set to 15 for the SGG-VG dataset. Moreover, the sampling number  $N$  is 2,000. We use the information content only from Visual Genome to distinguish common predicates and informative ones unless otherwise stated. For scene graph generation in the SGG-GQA dataset,  $M$  and  $N$  are set to 30 and 4000, respectively.

**Sentence-to-Graph Retrieval.** We follow the implementation of sentence-to-graph retrieval in Tang et al. (2020). This retrieval task is regarded as a matching problem between scene graphs and caption graphs. The SGG models trained in SGG-VG is used to extract image scene graphs. The caption graphs are constructed by an automatic method (Schuster et al., 2015) from image captions. The bilinear attention mechanism (Kim, Jun, & Zhang, 2018) maps caption graphs and image graphs into a 1024-d embedding space, and the triplet loss supervises the learning process. The training phase contains 30 epochs. The batch size and the learning rate are set to 12 and  $12 \times 10^{-2}$ , respectively.

**Image Captioning.** The image captioning task utilizes the code base of Luo, Price, Cohen, and Shakhnarovich (2018). We choose the Transformer Captioning model in the model zoo<sup>1</sup> as the baseline for the image captioning task. The SGG model trained by the SGG-GQA dataset extracts scene graphs in the image captioning dataset since the SGG-GQA dataset contains richer annotations than SGG-VG. For simplicity, we divide the scene graph into triplet labels, *i.e.*, (subject, predicate, object), and extract the top 128 triplets with the highest score for each image. The subject, predicate and object in a triplet are embedded to three 300-d vectors, respectively, and then concatenated

---

<sup>1</sup><https://github.com/ruotianluo/self-critical.pytorch>

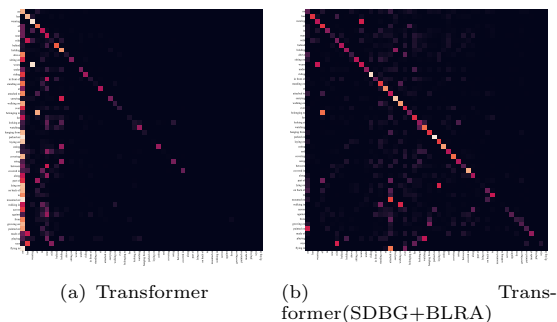


**Fig. 9** Confusion matrices of Transformer and Transformer (SDBG+BLRA). The coordinates of these matrices are arranged in the increasing order of predicate information content from left to right and top to bottom.

to a 900-d vector. The self-attention layer encodes the triplet embeddings, likely the operation of instance visual features in the model zoo. In the decoder, the current encoded word first queries the instance visual features with the multi-head attention layer and then queries the encoded triplets to predict the next word. The instance visual features are the bottom-up features and are downloaded from the codebase. The training phase contains 20 epochs. The batch size and the learning rate are set to 10 and  $5 \times 10^{-4}$ , respectively. The beam size is 5 for inference.

All experiments are conducted on a Ubuntu-20.04 server with 256G Memory, 2 Intel(R) Xeon(R) E5 CPUs and 8 TITAN Xp GPUs Cards. Our implementation is based on the PyTorch deep learning library.

## 4.4 Main Results

In this section, we investigate the superiority of our proposed method from four aspects: 1) performance of scene graph generation; 2) information content of predicate prediction; 3) accuracy of informative predicates; and 4) effectiveness of generated scene graphs on downstream tasks.

For scene graph generation, we investigate the generalization capability of our proposed method by adding it to three baseline models, *i.e.*, Transformer, MotifNet and VCTree. In Sect. 3, we design two sub-modules for both Semantic Debiasing and Balanced Predicate Learning, *i.e.*, Semantic Debiasing with Confusion Matrix (SDCM)/Bipartite Graph (SDBG), and Balanced Predicate Learning with Randomly Under-sampling (BLRU)/Removing Ambiguous Samples

(BLRA). These sub-modules are gradually added to the above baseline models.

The experimental results are summarized in Table 1. As can be seen, with respect to each baseline, our full method (**SDBG+BLRA**) achieves remarkable improvements of *at least* 100% for all subtasks and metrics. On the most challenging task SGDet, our full method achieves the largest improvements over the baselines. For instance, it achieves improvements of 161.0%, 150.9% and 141.2% on mR@20, mR@50, and mR@100 over vanilla MotifNet, respectively. Similar gains are obtained when applying our method to Transformer and VCTree, indicating its generalizability.

Moreover, combinations of our other sub-modules also achieve significant improvements. For instance, Transformer+BLRU outperforms the vanilla Transformer by 12.1 on mR@20 of PredCls (24.5 *vs.* 12.4). By removing ambiguous samples with BLRA, performance is further boosted to 27.9, which is 3.4 absolute points higher than BLRU. These results demonstrate two aspects: 1) ambiguous samples do seriously limit the performance of the model, and 2) our method effectively alleviates the impact of ambiguous samples. It is further improved (28.5 *vs.* 27.9) when SDCM is applied to improve informative predictions, using the confusion matrix. Finally, by constructing the bipartite graph with the subject-object overlap, the performance of Transformer increases to 29.3. These results show that the Semantic Debiasing module can help the model learn rich predicate information and our predicate relationship structure is effective.

Besides SGG-VG, we verify our method for the scene graph generation task on a more challenging dataset, SGG-GQA. We also need the model trained in SGG-GQA to generate scene graphs for the image captioning task since SGG-GQA contains more object and predicate categories than those of SGG-VG. Therefore, to save time, we flexibly choose the combination of BLRU and SDBG, which do not need to infer the training data compared with BLRA and SDCM. As shown in Table 3, Transformer (SDBG+BLRU) achieves higher scores than vanilla Transformer (*e.g.*, 1.58 *vs.* 2.68 on mR@20). This result illustrates that our method is competent for complex environments (1704 object categories and 311 predicate categories).

**Table 1** Main evaluation results on the generalizability and effectiveness of our proposed components, *i.e.*, Balanced Predicate Learning (BPL) and Semantic Debiasing (SD). The proposed method is applied to three baseline models, where the MotifNet and VCTree are reimplemented by Tang et al. (2020).

Method	PredCls			SGCls			SGDet		
	mR@20	mR@50	mR@100	mR@20	mR@50	mR@100	mR@20	mR@50	mR@100
Transformer	12.4	16.0	17.5	7.7	9.6	10.2	5.3	7.3	8.8
Transformer+BLRU	24.5	29.4	31.7	14.1	16.8	17.8	10.2	13.2	15.4
Transformer+BLRA	27.9	34.0	36.6	16.0	19.2	20.4	10.6	14.0	16.7
Transformer+SDCM+BLRA	28.5	34.1	36.4	16.4	19.2	20.4	11.4	14.8	17.3
Transformer+SDBG+BLRA	29.3	34.7	36.8	16.9	19.5	20.5	11.8	15.2	17.8
MotifNet	11.5	14.6	15.8	6.5	8.0	8.5	4.1	5.5	6.8
MotifNet+BLRU	22.6	27.1	29.1	13.0	15.3	16.2	9.7	12.4	14.4
MotifNet+BLRA	25.5	30.8	33.2	14.2	16.9	17.8	9.7	12.7	15.1
MotifNet+SDCM+BLRA	26.0	31.3	33.3	14.4	17.1	17.9	10.4	13.4	15.7
MotifNet+SDBG+BLRA	27.1	31.9	33.8	14.8	17.6	18.3	10.7	13.8	16.4
VCTree	11.7	14.9	16.1	6.2	7.5	7.9	4.2	5.7	6.9
VCTree+BLRU	23.8	28.4	30.4	15.6	18.4	19.5	9.9	12.5	14.4
VCTree+BLRA	27.1	32.5	34.6	17.4	20.8	22.0	9.7	12.6	14.8
VCTree+SDCM+BLRA	27.7	32.6	34.5	17.8	21.0	22.1	10.3	13.2	15.4
VCTree+SDBG+BLRA	28.6	33.2	34.9	18.4	21.4	22.4	10.5	13.6	15.9

**Table 2** Information content assessment on PredCls. Models are evaluated on two information sources (Visual Genome & Wikipedia). TF denotes Transformer.

Metric	Method	mRIC@20	mRIC@50	mRIC@100
mRIC (VG)	TF	43.5	59.2	65.8
	TF+BLRU	118.2	142.6	154.5
	TF+BLRA	145.2	178.1	192.9
	TF+SDCM+BLRA	152.5	183.5	196.7
	TF+SDBG+BLRA	159.1	189.3	201.1
mRIC (Wiki)	TF	74.1	96.6	105.9
	TF+BLRU	182.1	216.3	231.3
	TF+BLRA	211.9	253.4	270.8
	TF+SDCM+BLRA	222.2	262.0	277.5
	TF+SDBG+BLRA	231.3	270.0	283.9

**Table 3** Comparison of Transformer and Transformer (SDBG+BLRU) on SGDet in the SGG-GQA dataset.

Models	mR@20	mR@50	mR@100
Transformer	1.58	2.12	2.48
Transformer (SDBG+BLRU)	2.68 <sup>+1.10</sup>	3.35 <sup>+1.23</sup>	3.81 <sup>+1.33</sup>

To evaluate whether our DB-SGG framework can provide more informative content, we report evaluation results on mRIC@K for Transformer on SGG-VG. The evaluation results based on the two information sources (Visual Genome and Wikipedia) are summarized in Table 2. From the table, we can observe that DB-SGG obtains higher scores when compared with Transformer, which demonstrates that our method generates more informative scene graphs.

Moreover, To evaluate whether our DB-SGG framework can provide more informative content, we report evaluation results on mRIC@K for Transformer on SGG-VG. The evaluation results based on the two information sources

**Table 4** Comparison of Transformer and Transformer (SDBG+BLRA) on sentence-to-graph retrieval.

Gallery Size	R@K	Transformer	Transformer (SDBG+BLRA)
1000	R@20	14.4	21.3 <sup>+6.9</sup>
	R@50	26.4	35.6 <sup>+9.2</sup>
	R@100	35.9	48.3 <sup>+12.4</sup>
5000	R@20	3.8	6.3 <sup>+2.5</sup>
	R@50	8.4	13.1 <sup>+4.7</sup>
	R@100	14.5	21.5 <sup>+7.0</sup>

**Table 5** Comparison of Transformer and Transformer (SDBG+BLRU) on image captioning. BL means the baseline captioning model. TF means the Transformer SGG model.

Models	Bleu-4	Meteor	Cider	Spice
BL	35.5	27.8	112.6	20.6
BL+TF	35.5	27.9	112.8	20.7
BL+TF (SDBG+BLRU)	35.5	27.8	113.7	20.9

(Visual Genome and Wikipedia) are summarized in Table 2. From the table, we can observe that DB-SGG obtains higher scores when compared with Transformer, which demonstrates that our method generates more informative scene graphs.

In order to intuitively show the accuracy of informative predicates, we visualize confusion matrices across predicate categories. In particular, we compare two confusion matrices generated from Transformer and our method in Fig. 9. Not surprisingly, our proposed method detects more informative predicates much more accurately than

**Table 6** Ablation studies of adjusted domain construction in BPL.

Target Domain	SGG (PredCls)			mRIC (VG)			mRIC (Wiki)		
	mR@20	mR@50	mR@100	mRIC@20	mRIC@50	mRIC@100	mRIC@20	mRIC@50	mRIC@100
- (original domain)	12.4	16.0	17.5	43.5	59.2	65.8	74.1	96.6	105.9
Wikipedia	21.3	26.0	28.0	99.5	121.9	131.5	166.1	198.4	211.7
Visual Genome	26.7	31.9	34.2	134.5	160.3	172.5	204.6	239.2	254.4

**Table 7** Ablation studies of the transition matrix on PredCls.

Settings	$C^*$	finetune	mR@20	mR@50	mR@100
1	-	-	24.5	29.4	31.7
2	RM	✓	25.1	29.5	31.3
3	CM	✓	25.8	30.2	32.1
4	CM	-	26.7	31.9	34.2
5	CCM	-	25.2	30.0	32.1
6	SOO	-	26.0	31.2	33.4
7	SOBG	-	27.8	33.5	36.1

**Table 8** Parameter sensitivity analysis of  $\alpha$  in Equation (4) on PredCls.

$\alpha$	mR@20	mR@50	mR@100
$\alpha = 0.0$	20.5	25.4	27.3
$\alpha = 0.3$	25.8	30.5	32.8
$\alpha = 0.6$	26.4	31.6	33.9
$\alpha = 1.0$	26.7	31.9	34.2

**Table 9** Analysis of the number of common predicates  $N$  in the adjusted domain.

$N$	mR@20	mR@50	mR@100
$N = 2k$	24.5	29.4	31.7
$N = 4k$	22.7	27.4	29.5
$N = 6k$	21.7	26.1	28.1
$N = 8k$	20.7	25.0	27.1

the Transformer since the confusion matrix generated from the proposed method is much brighter on the diagonal than that of the Transformer. Besides, Transformer (SDBG+BLRA) effectively handles common predicates, as its brightest elements are no longer concentrated on the left, compared with the confusion matrix of the Transformer.

As for the practicability of generated scene graphs, we show the S2G (Sentence to Graph) retrieval task in Table 4. The scene graphs generated from Transformer (SDBG+BLRA) retrieve more correct results than that of Transformer (*e.g.*, 3.8 *vs.* 6.3 on R@20 in the 5*k* gallery). Therefore, the scene graphs generated by our method can fully represent the image content.

After training in SGG-GQA, we use the trained model to generate scene graphs for the image captioning task. As shown in Table 5, the baseline uses the scene graphs generated by the

**Table 10** Analysis of the number of common predicates  $M$  in the adjusted domain.

$M$	mR@20	mR@50	mR@100
$M = 5$	21.5	25.7	27.5
$M = 10$	24.3	29.3	31.4
$M = 15$	24.5	29.4	31.7
$M = 20$	24.3	29.2	31.5

**Table 11** Ablation studies of training approaches on PredCls. F-backbone means that the backbone before the classifier layer of an SGG model is finetuned.

Settings	pre-trained	F-backbone	R@20	R@50	R@100
1	-	-	28.4	34.9	37.2
2	✓	✓	30.6	37.3	39.5
3	✓	-	49.0	55.7	57.6

**Table 12** Compared with TDE on PredCls (Mean Recall). TF denotes Transformer.

Settings	mR@20	mR@50	mR@100
TF	12.4	16.0	17.5
TF+TDE	16.2	23.4	27.6
TF+BLRU	24.5	29.4	31.7
TF+BLRU+TDE	21.5	29.0	33.2
TF+SDCM+BLRU	26.7	31.9	34.2
TF+SDBG+BLRU	27.8	33.5	36.1

vanilla Transformer without significant improvement. However, the scene graphs generated by Transformer (SDBG+BLRU) improve the baseline on Cider (112.6 *vs.* 113.7). Since Cider highlights informative words weighted by TF-IDF in image captions, the improvement on Cider undoubtedly clarifies the informativeness of the scene graphs generated by our method.

## 4.5 Ablation Study on Details of Proposed Method

In this section, we investigate variants of our method for more insights. We study the two variants of each of our proposed sub-modules: SD and BPL. We use the Transformer as the baseline in the following experiments. Since we have compared BLRU/BLRA and SDCM/SDBG in the previous section, the main experimental subject in this section is Transformer (**SDCM+BLRU**) unless otherwise stated.

**Variants to SD.** For SD, we investigate variants of the transition matrix, *i.e.*,  $C^*$  in Equation (4). In particular, we compare seven settings: 1) Transformer model with BPL but without SD, which is the baseline. 2)  $C^*$  implemented by a Random Matrix (RM) and updated during training (*i.e.*, a randomly initialized linear layer  $W \in \mathbb{R}^{P \times P}$ , where  $P$  denotes the amounts of predicate categories). 3)  $C^*$  calculated by the Confusion Matrix (CM, Sect. 3.2.1) and updated during training (*i.e.*, a learnable linear layer  $W$  initialized as the Confusion Matrix). 4)  $C^*$  calculated by the Confusion Matrix (CM, Sect. 3.2.1) and fixed during training. 5)  $C^*$  calculated by the transpose of the Column-normalized Confusion Matrix (CCM, Sect. 3.2.1) and fixed during training. 6)  $C^*$  calculated by the Subject-Object Overlap (SOO) without the bipartite graph constraint (Sect. 3.2.2). 7)  $C^*$  calculated by the Subject-Object Bipartite Graph (SOBG, Sect. 3.2.2). The experimental results are shown in Table 7. From the results, we can make the following observations. The transition matrix initialized from a random matrix and updated during training (setting 2) brings minor gains in terms of mean recall scores. The fixed transition matrix (setting 4) obtained from prediction priors (*i.e.*, Equation (4)) performs better than when it is updated (setting 3). This implies updating the transition matrix during training hurts the quality of the common-to-informative debiasing process, leading to sub-optimal results. The row-normalized confusion matrix is better than the column-normalized one by comparing CM (setting 4) and CCM (setting 5), verifying that the predicate relationship in the row-normalized matrix is more evident, as mentioned in Sect. 3.2.1. Compared with the confusion matrix, directly using the subject-object overlap (setting 6) does not further enhance the model because the confusion matrix already presents an approximate bipartite structure from common predicates to informative ones, as shown in Fig. 1(a). When we constrain the subject-object overlap to the bipartite graph (setting 7), the scores are higher than those of CM (setting 4) and SOO (setting 6), which means that the bipartite graph is necessary for constructing the semantic relationship.

**Parameter sensitivity analysis of  $\alpha$ .** In Equation (4), we add an identity matrix and introduce a hyper-parameter  $\alpha$ . The adjustment of  $\alpha$

is shown in Table 8. From Table 8, we can see that the model not only needs to add the identity matrix, but also needs to set  $\alpha$  equal to 1 to obtain the best results.

**Variants to BPL.** As illustrated in Sect. 3.3, the proposed BPL learning process consists of three steps, in which the construction of the adjusted domain is the essential part. To create the adjusted domain, an information source is needed to calculate information content (IC) for each predicate category. Based on their IC values, predicates are further categorized as common or informative. Here we use two different sources for IC calculation: 1) Visual Genome, which provides triplets for visual contents; and 2) Wikipedia, which provides a large textual corpus (about 110k). Notably, Wikipedia is a language-based corpus without visual contents. Two adjusted domains are generated based on these two information sources. We perform diagnostic experiments to investigate whether SGG models can benefit from the adjusted domain, which is a more balanced sample space. In particular, we compare three settings: 1) Transformer model trained on the original domain. 2) Transformer model trained on the adjusted domain based on Wikipedia. 3) Transformer model trained on the adjusted domain based on Visual Genome. The experimental results are summarized in Table 6, from which we have the following findings. First, SGG models trained on the adjusted domain, either language-based or visual-based, outperform the one trained on the original domain by a large margin (at least 8.9 absolute points gains for mR@20). This indicates a balanced sample space plays an important role in training the SGG model. Besides, the SGG model is also improved after being trained on the language-based adjusted domain, demonstrating the effectiveness and generalizability of the proposed IC-based predicate partition. As for the assessment of information contents (mRIC@k), models trained on the adjusted domains achieve higher scores than the model trained on the original domain. This demonstrates that the scene graphs generated from the models trained on the adjusted domains provide more informative content for better scene understanding.

**Variants to number of common predicates  $N$ .** We examine how the number of common predicate examples ( $N$  in Sect. 3.3.1) in the adjusted domain affects model performance. We increase

$N$  from  $2k$  to  $8k$  in Table 9. The performance of the model decreases gradually with the increase of  $N$ . Thus, allocating too many samples for common predicates is harmful to predicting abundant predicates. We further examine how the number of common predicate categories ( $M$  in Sect. 3.3.1) affects model performance, as shown in Table 10. When  $M = 15$ , the model achieves the best results. Too many or too few common predicates are not conducive to the learning process. The adjustments of  $N$  and  $M$  are based on Transformer (BLRU).

**Variants to training approaches.** After the construction of the adjusted domain, an effective training approach is needed. To explore this aspect, we perform an additional experiment as illustrated in Table 11, where it compares three different training settings: 1) Training an SGG model from scratch on the adjusted domain, 2) Finetuning an SGG model on the adjusted domain, where it is pre-trained on the original domain, and 3) Finetuning the classifier layer of an SGG model on the adjusted domain, where it is pre-trained on the original domain. From Table 11, we can observe that the third setting provides the best result, whilst directly training an SGG model from scratch on the adjusted domain gives the worst result. Furthermore, the SGG model trained with the third setting substantially outperforms the one trained with the second setting. One possible reason is that the scale of sample space in the adjusted domain (about  $55k$ ) is much smaller than that of the original domain (about  $400k$ ), posing high risks of overfitting.

**Comparison with TDE.** We also compare our method and TDE (Tang et al., 2020) in Table 12 carefully. Although TDE can boost Transformer, BLRU achieves higher scores than TDE (24.5 vs. 16.2). Moreover, TDE is hard to improve the model after BLRU by comparing Transformer+BLRU and Transformer+BLRU+TDE (24.5 vs. 21.5) since BLRU already provides unbiased results and TDE cannot fully use its visually unbiased advantages. SDCM and SDBG further enhance the model after BLRU (26.7 vs. 24.5 and 27.8 vs. 24.5) since the semantic debiasing of SDCM and SDBG assists the data debiasing of BLRU.

## 4.6 Comparison with State-of-the-art Methods

After verifying the effect of our proposed DB-SGG framework, we compare it with state-of-the-art SGG models. The comparison results are shown in Table 13. As can be seen, DB-SGG achieves the best performance on all metrics among all the comparison methods, reaching 29.3 mR@20 for PredCls, 16.9 mR@20 for SGCl and 11.8 mR@20 for SGGDet, respectively. Specifically, when being compared with state-of-the-art debiasing method, *i.e.*, Cogtree (Yu et al., 2021), our method outperforms it on three baselines (*i.e.*, MotifNet, Transformer and VCTree) with consistent improvements as 6.2, 6.4 and 6.6 on mR@20 for PredCls, respectively. Similar gains are also observed for the other two tasks. Compared with the resample or reweight methods, *e.g.*, MotifNet (Focal), MotifNet (Reweight) and MotifNet (Resample), our method also outperforms them, as they do not simultaneously consider the two types of imbalances, *i.e.*, semantic space level imbalance and training sample level imbalance. This experiment clearly demonstrates the superiority of our method and the significance of the two imbalances.

## 4.7 Visualization Results

We first compare the Transformer with the Transformer equipped with our proposed method (DB-SGG). From Fig. 10, it can be seen that Transformer (SDBG+BLRU) generates more informative scene graphs than vanilla Transformer, *e.g.*, (man, sitting on, bed) *vs.* (man, on, bed) in the first example, (car, parked on, street) *vs.* (car, on, street) in the second example, and (1-flower, painted on, vase) *vs.* (1-flower, in, vase) in the third example. In the fourth example, Transformer only gives higher scores for some common relationships, *e.g.*, (cat, has, 1-ear) and (1-ear, of, cat), and fails to detect significant instances of interactions. Different from the baseline, some important interactions also achieve high scores in our Transformer (SDBG+BLRU), *e.g.*, (cat, looking at, screen) and (screen, behind, cat). These results clearly demonstrate the success of predicates debiasing by our proposed method.

Moreover, we explore our method in various scenarios, from simple to complex. As shown in Fig. 11, our method handles all simple scenarios



**Table 13** Comparison between our method (DB-SGG) and previous methods.

Method	PredCls			SGCls			SGDet		
	mR@20	mR@50	mR@100	mR@20	mR@50	mR@100	mR@20	mR@50	mR@100
IMP+ (T. Chen et al., 2019; Xu et al., 2017)	-	9.8	10.5	-	5.8	6.0	-	3.8	4.8
FREQ (Tang et al., 2019; Zellers et al., 2018)	8.3	13.0	16.0	5.1	7.2	8.5	4.5	6.1	7.1
KERN (T. Chen et al., 2019)	-	17.7	19.2	-	9.4	10.0	-	6.4	7.3
GPS-Net (X. Lin et al., 2020)	-	-	22.8	-	-	12.6	-	-	9.8
GB-Net (Zareian, Karaman, & Chang, 2020)	-	22.1	24.0	-	12.7	13.4	-	7.1	8.5
MotifNet (Tang et al., 2020; Zellers et al., 2018)	11.5	14.6	15.8	6.5	8.0	8.5	4.1	5.5	6.8
MotifNet (Focal) (Tang et al., 2020; Zellers et al., 2018)	10.9	13.9	15.0	6.3	7.7	8.3	3.9	5.3	6.6
MotifNet (Reweight) (Tang et al., 2020; Zellers et al., 2018)	16.0	20.0	21.9	8.4	10.1	10.9	6.5	8.4	9.8
MotifNet (Resample) (Tang et al., 2020; Zellers et al., 2018)	14.7	18.5	20.0	9.1	11.0	11.8	5.9	8.4	9.8
MotifNet (TDE) (Tang et al., 2020; Zellers et al., 2018)	18.5	24.9	28.3	11.1	13.9	15.2	6.6	8.5	9.9
MotifNet (CogTree) (Yu et al., 2021; Zellers et al., 2018)	20.9	26.4	29.0	12.1	14.9	16.1	7.9	10.4	11.8
VCTree (Tang et al., 2020, 2019)	11.7	14.9	16.1	6.2	7.5	7.9	4.2	5.7	6.9
VCTree (TDE) (Tang et al., 2020, 2019)	18.4	25.4	28.7	8.9	12.2	14.0	6.9	9.3	11.1
VCTree (CogTree) (Tang et al., 2019; Yu et al., 2021)	22.0	27.6	29.7	15.4	18.8	19.9	7.8	10.4	12.1
Transformer (CogTree) (Yu et al., 2021)	22.9	28.4	31.0	13.0	15.7	16.7	7.9	11.1	12.7
MotifNet (SDBG+BLRA)	<b>27.1</b>	<b>31.9</b>	<b>33.8</b>	<b>14.8</b>	<b>17.6</b>	<b>18.3</b>	<b>10.7</b>	<b>13.8</b>	<b>16.4</b>
VCTree (SDBG+BLRA)	<b>28.6</b>	<b>33.2</b>	<b>34.9</b>	<b>18.4</b>	<b>21.4</b>	<b>22.4</b>	<b>10.5</b>	<b>13.6</b>	<b>15.9</b>
Transformer (SDBG+BLRA)	<b>29.3</b>	<b>34.7</b>	<b>36.8</b>	<b>16.9</b>	<b>19.5</b>	<b>20.5</b>	<b>11.8</b>	<b>15.2</b>	<b>17.8</b>

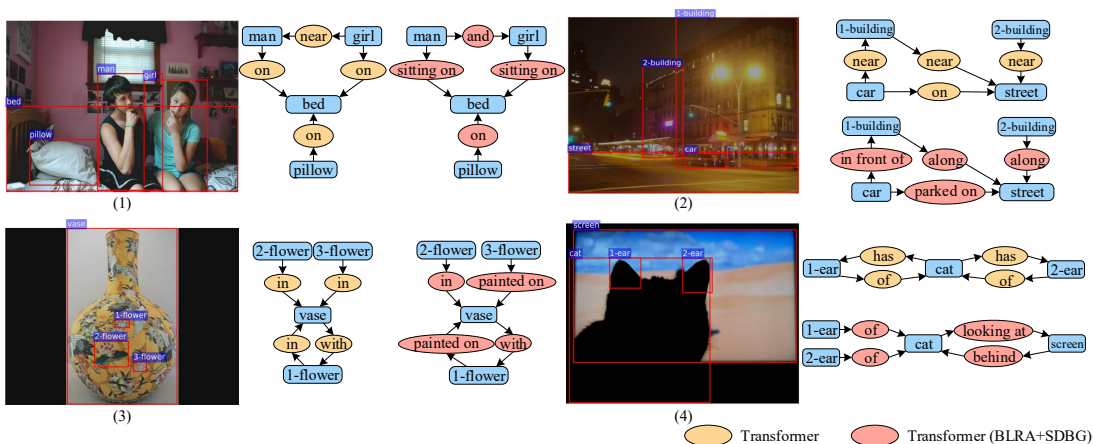


**Fig. 10** Visualization results of Transformer and Transformer (SDBG+BLRA) on the PredCls task. The generated scene graph from the Transformer (SDBG+BLRA) is more informative than the one from Transformer. Only top 30% relationships on each image are shown for clarity.

successfully, *e.g.*, (1-horse, near, 2-horse) in the first example, (food, on, plate) in the third example and (bird, has, tail) in the fourth example. For the fifth image, some complex spatial relationships are accurately identified by our method, *e.g.*, (tree, in front of, building) and (tree, behind, man). Our method also generates a complete scene graph for the more complicated situation in the sixth example. However, this example has some unreasonable relationships, *e.g.*, (railing, attached to, tree), because our method is too radical in choosing more common predicates, such as “near” or “under”. Therefore, balancing stability and informativeness effectively for scene graph generation is an essential problem in future work.

## 5 Conclusion

In this work, we propose the DB-SGG framework based on debiasing for informative scene graph generation. We first delineate two types of imbalance between common predicates and informative ones. Two strategies are designed: Semantic Debiasing (SD) and Balanced Predicate Learning (BPL), in view of the imbalance. SD explores the semantic relationship between predicates with the confusion matrix and the bipartite graph. BPL transfers the knowledge learned from general predicates to informative ones with the random undersampling strategy and the ambiguity removing strategy. It is worth noting that DB-SGG can be readily integrated with existing SGG models to improve their performances. Finally, comprehensive experiments on two SGG

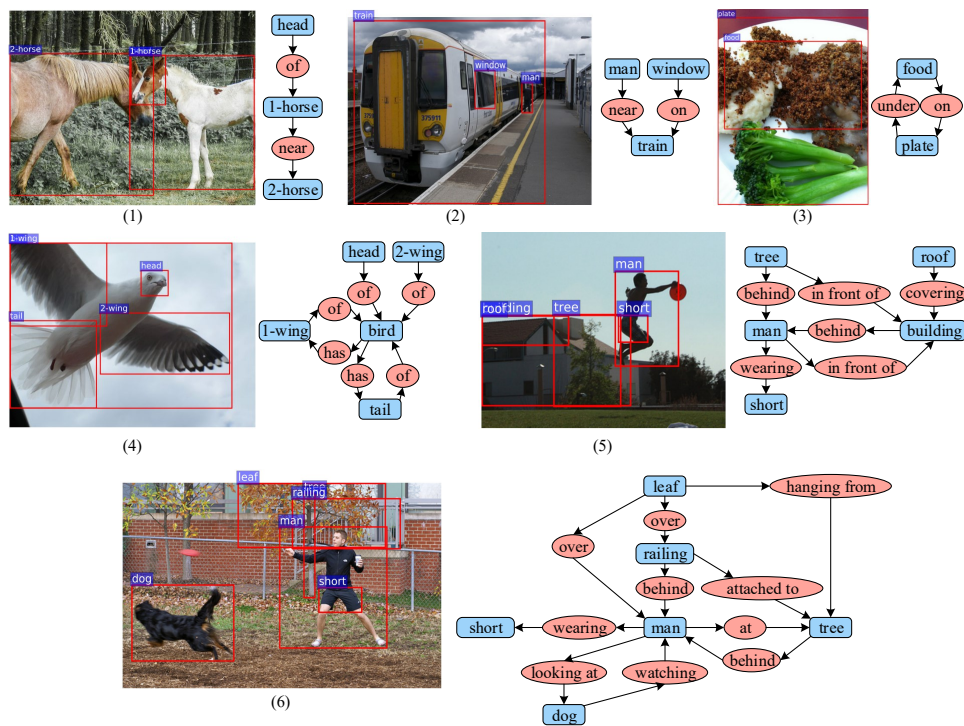


**Fig. 11** Visualization results of Transformer (SDBG+BLRA) on the PredCls task for various scenarios. Only top 30% relationships on each image are shown for clarity.

datasets and two downstream tasks demonstrate that our method improves the informativeness of generated scene graphs and outperforms state-of-the-art SGG models significantly.

## 6 Declarations

**Funding** This study was supported by Kuaishou.

**Competing interests** The authors have no other competing interests to disclose.

**Data availability** The datasets generated and analysed during the current study are available in the Visual Genome repository <https://visualgenome.org/>.

## References

Anderson, P., Fernando, B., Johnson, M., Gould, S. (2016). SPICE: semantic propositional image caption evaluation. *European conference on computer vision* (Vol. 9909, pp. 382–398).

Anderson, P., He, X., Buehler, C., Teney, D., Johnson, M., Gould, S., Zhang, L.

(2018). Bottom-up and top-down attention for image captioning and visual question answering. *IEEE conference on computer vision and pattern recognition* (pp. 6077–6086).

Chen, L., Zhang, H., Xiao, J., He, X., Pu, S., Chang, S. (2019). Counterfactual critic multi-agent training for scene graph generation. *IEEE international conference on computer vision* (pp. 4612–4622).

Chen, M., Lyu, X., Guo, Y., Liu, J., Gao, L., Song, J. (2022). Multi-scale graph attention network for scene graph generation. *Icme*.

Chen, T., Yu, W., Chen, R., Lin, L. (2019). Knowledge-embedded routing network for scene graph generation. *IEEE conference on computer vision and pattern recognition* (pp. 6163–6171).

Chen, Y., Bai, Y., Zhang, W., Mei, T. (2019). Destruction and construction learning for

- fine-grained image recognition. *IEEE conference on computer vision and pattern recognition* (pp. 5157–5166).
- Cohn-Gordon, R., Goodman, N.D., Potts, C. (2018). Pragmatically informative image captioning with character-level inference. (pp. 439–443).
- Denkowski, M.J., & Lavie, A. (2014). Meteor universal: Language specific translation evaluation for any target language. *Acl workshop* (pp. 376–380).
- Girshick, R.B. (2015). Fast R-CNN. *IEEE international conference on computer vision* (pp. 1440–1448).
- Girshick, R.B., Donahue, J., Darrell, T., Malik, J. (2016). Region-based convolutional networks for accurate object detection and segmentation. *IEEE Transactions on Pattern Analysis and Machine Intelligence*, 38(1), 142–158.
- Gu, J., Zhao, H., Lin, Z., Li, S., Cai, J., Ling, M. (2019). Scene graph generation with external knowledge and image reconstruction. *IEEE conference on computer vision and pattern recognition* (pp. 1969–1978).
- Guo, W., Zhang, Y., Yang, J., Yuan, X. (2021). Re-attention for visual question answering. *IEEE Transactions on Image Processing*, 30, 6730–6743.
- Guo, Y., Gao, L., Wang, X., Hu, Y., Xu, X., Lu, X., ... Song, J. (2021). From general to specific: Informative scene graph generation via balance adjustment. *IEEE international conference on computer vision* (p. 16383-16392).
- Guo, Y., Song, J., Gao, L., Shen, H.T. (2020). One-shot scene graph generation. *Acm international conference on multimedia* (pp. 3090–3098).
- He, K., Zhang, X., Ren, S., Sun, J. (2016). Deep residual learning for image recognition. *IEEE conference on computer vision and pattern recognition* (pp. 770–778).
- Herzig, R., Raboh, M., Chechik, G., Berant, J., Globerson, A. (2018). Mapping images to scene graphs with permutation-invariant structured prediction. *Neural information processing systems* (pp. 7211–7221).
- Hudson, D.A., & Manning, C.D. (2019). GQA: A new dataset for real-world visual reasoning and compositional question answering. *IEEE conference on computer vision and pattern recognition* (pp. 6700–6709).
- Hung, Z.-S., Mallya, A., Lazebnik, S. (2020). Contextual translation embedding for visual relationship detection and scene graph generation. *IEEE Transactions on Pattern Analysis and Machine Intelligence*, 43(11), 3820–3832.
- Johnson, J., Krishna, R., Stark, M., Li, L., Shamma, D.A., Bernstein, M.S., Li, F. (2015). Image retrieval using scene graphs. *IEEE conference on computer vision and pattern recognition* (pp. 3668–3678).
- Kan, X., Cui, H., Yang, C. (2021). Zero-shot scene graph relation prediction through common-sense knowledge integration. N. Oliver, F. Pérez-Cruz, S. Kramer, J. Read, & J.A. Lozano (Eds.), *Pkdd*.
- Kan, X., Cui, H., Yang, C. (2022). Zero-shot predicate prediction for scene graph parsing. Y. Li, X. Yang, X. Huang, Z. Ma, & C. Xu (Eds.), *Tmm*.
- Kim, J., Jun, J., Zhang, B. (2018). Bilinear attention networks. *Neural information processing systems* (pp. 1571–1581).
- Krishna, R., Zhu, Y., Groth, O., Johnson, J., Hata, K., Kravitz, J., ... Fei-Fei, L. (2017). Visual genome: Connecting language and vision using crowdsourced dense image annotations. *International Journal of Computer Vision*, 123(1), 32–73.

- Lam, M., Mahasseni, B., Todorovic, S. (2017). Fine-grained recognition as hsnet search for informative image parts. *IEEE conference on computer vision and pattern recognition* (pp. 6497–6506).
- Li, R., Zhang, S., He, X. (2022). SGTR: end-to-end scene graph generation with transformer. *Cvpr*.
- Li, R., Zhang, S., Wan, B., He, X. (2021). Bipartite graph network with adaptive message passing for unbiased scene graph generation. *Cvpr*.
- Li, X., Song, J., Gao, L., Liu, X., Huang, W., He, X., Gan, C. (2019). Beyond rnns: Positional self-attention with co-attention for video question answering. *Association for the advancement of artificial intelligence* (pp. 8658–8665).
- Li, Y., Ouyang, W., Zhou, B., Shi, J., Zhang, C., Wang, X. (2018). Factorizable net: An efficient subgraph-based framework for scene graph generation. *European conference on computer vision* (Vol. 11205, pp. 346–363).
- Liang, C., Wu, Z., Huang, W., Giles, C.L. (2015). Measuring prerequisite relations among concepts. (pp. 1668–1674).
- Liang, Y., Bai, Y., Zhang, W., Qian, X., Zhu, L., Mei, T. (2019). Vrr-vg: Refocusing visually-relevant relationships. *IEEE international conference on computer vision* (pp. 10402–10411).
- Lin, D. (1998). An information-theoretic definition of similarity. (pp. 296–304).
- Lin, T., Dollár, P., Girshick, R.B., He, K., Hariharan, B., Belongie, S.J. (2017). Feature pyramid networks for object detection. *IEEE conference on computer vision and pattern recognition* (pp. 936–944).
- Lin, T., Maire, M., Belongie, S.J., Hays, J., Perona, P., Ramanan, D., ... Zitnick, C.L. (2014). Microsoft COCO: common objects in context. D.J. Fleet, T. Pajdla, B. Schiele, & T. Tuytelaars (Eds.), *European conference on computer vision* (Vol. 8693, pp. 740–755).
- Lin, X., Ding, C., Zeng, J., Tao, D. (2020). Gps-net: Graph property sensing network for scene graph generation. *IEEE conference on computer vision and pattern recognition* (pp. 3743–3752).
- Liu, H., Yan, N., Mortazavi, M.S., Bhanu, B. (2021). Fully convolutional scene graph generation. *Cvpr*.
- Lu, C., Krishna, R., Bernstein, M.S., Li, F. (2016). Visual relationship detection with language priors. *European conference on computer vision* (Vol. 9905, pp. 852–869).
- Luo, R., Price, B.L., Cohen, S., Shakhnarovich, G. (2018). Discriminability objective for training descriptive captions. *IEEE conference on computer vision and pattern recognition* (pp. 6964–6974).
- Lyu, X., Gao, L., Guo, Y., Zhao, Z., Huang, H., Shen, H.T., Song, J. (2022). Fine-grained predicates learning for scene graph generation. *Cvpr*.
- Lyu, X., Gao, L., Xie, J., Zeng, P., Tian, Y., Shao, J., Shen, H.T. (2023). Generalized unbiased scene graph generation. *Corr*.
- Lyu, X., Gao, L., Zeng, P., Shen, H.T., Song, J. (2022). Adaptive fine-grained predicates learning for scene graph generation. *TPAMI*.
- Lyu, X., Liu, J., Guo, Y., Gao, L. (2023). Local-global information interaction debiasing for dynamic scene graph generation. *Corr*.
- McMahon, D. (2007). *Quantum computing explained*.
- Mi, L., & Chen, Z. (2020). Hierarchical graph attention network for visual relationship detection. *IEEE conference on computer*

- vision and pattern recognition* (pp. 13883–13892).
- Newell, A., & Deng, J. (2017). Pixels to graphs by associative embedding. *Neural information processing systems* (pp. 2171–2180).
- Papineni, K., Roukos, S., Ward, T., Zhu, W. (2002). Bleu: a method for automatic evaluation of machine translation. (pp. 311–318).
- Pedersen, T. (2010). Information content measures of semantic similarity perform better without sense-tagged text. (pp. 329–332).
- Redmon, J., Divvala, S.K., Girshick, R.B., Farhadi, A. (2016). You only look once: Unified, real-time object detection. *IEEE conference on computer vision and pattern recognition* (pp. 779–788).
- Ren, S., He, K., Girshick, R.B., Sun, J. (2017). Faster R-CNN: towards real-time object detection with region proposal networks. *IEEE Transactions on Pattern Analysis and Machine Intelligence*, 39(6), 1137–1149.
- Resnik, P. (1995). Using information content to evaluate semantic similarity in a taxonomy. *International joint conference on artificial intelligence* (pp. 448–453).
- Resnik, P. (1999). Semantic similarity in a taxonomy: An information-based measure and its application to problems of ambiguity in natural language. *Journal of Artificial Intelligence Research*, 11, 95–130.
- Robertson, S. (2004). Understanding inverse document frequency: on theoretical arguments for IDF. *J. Documentation*, 60(5), 503–520.
- Ross, S. (2014). *A first course in probability*.
- Salton, G., & Buckley, C. (1988). Term-weighting approaches in automatic text retrieval. *Inf. Process. Manag.*, 24(5), 513–523.
- Schuster, S., Krishna, R., Chang, A.X., Fei-Fei, L., Manning, C.D. (2015). Generating semantically precise scene graphs from textual descriptions for improved image retrieval. *Emnlp workshop* (pp. 70–80).
- Seco, N., Veale, T., Hayes, J. (2004). An intrinsic information content metric for semantic similarity in wordnet. *Ecai* (pp. 1089–1090).
- Shen, F., Zhou, X., Yang, Y., Song, J., Shen, H.T., Tao, D. (2016). A fast optimization method for general binary code learning. *IEEE Transactions on Image Processing*, 25(12), 5610–5621.
- Song, J., Zhang, H., Li, X., Gao, L., Wang, M., Hong, R. (2018). Self-supervised video hashing with hierarchical binary auto-encoder. *IEEE Transactions on Image Processing*, 27(7), 3210–3221.
- Suhail, M., Mittal, A., Siddiquie, B., Broaddus, C., Eledath, J., Medioni, G.G., Sigal, L. (2021). Energy-based learning for scene graph generation. *Cvpr*.
- Tang, K. (2020). *A scene graph generation codebase in pytorch*. (<https://github.com/KaihuaTang/Scene-Graph-Benchmark.pytorch>)
- Tang, K., Niu, Y., Huang, J., Shi, J., Zhang, H. (2020). Unbiased scene graph generation from biased training. *IEEE conference on computer vision and pattern recognition* (pp. 3713–3722).
- Tang, K., Zhang, H., Wu, B., Luo, W., Liu, W. (2019). Learning to compose dynamic tree structures for visual contexts. *IEEE conference on computer vision and pattern recognition* (pp. 6619–6628).
- Teney, D., Liu, L., van den Hengel, A. (2017). Graph-structured representations for visual question answering. *IEEE conference on computer vision and pattern recognition* (pp. 3233–3241).

- Vaswani, A., Shazeer, N., Parmar, N., Uszkoreit, J., Jones, L., Gomez, A.N., ... Polosukhin, I. (2017). Attention is all you need. *Neural information processing systems* (pp. 5998–6008).
- Vedantam, R., Bengio, S., Murphy, K., Parikh, D., Chechik, G. (2017). Context-aware captions from context-agnostic supervision. *IEEE conference on computer vision and pattern recognition* (pp. 1070–1079).
- Vedantam, R., Zitnick, C.L., Parikh, D. (2015). Cider: Consensus-based image description evaluation. *IEEE conference on computer vision and pattern recognition* (pp. 4566–4575).
- Wang, S., Gao, L., Lyu, X., Guo, Y., Zeng, P., Song, J. (2022). Dynamic scene graph generation via temporal prior inference. *Mm*.
- Wang, Y., Morariu, V.I., Davis, L.S. (2018). Learning a discriminative filter bank within a CNN for fine-grained recognition. *IEEE conference on computer vision and pattern recognition* (pp. 4148–4157).
- Xie, S., Girshick, R.B., Dollár, P., Tu, Z., He, K. (2017). Aggregated residual transformations for deep neural networks. *IEEE conference on computer vision and pattern recognition* (pp. 5987–5995).
- Xu, D., Zhu, Y., Choy, C.B., Fei-Fei, L. (2017). Scene graph generation by iterative message passing. *IEEE conference on computer vision and pattern recognition* (pp. 3097–3106).
- Yao, T., Pan, Y., Li, Y., Qiu, Z., Mei, T. (2017). Boosting image captioning with attributes. *IEEE international conference on computer vision* (pp. 4904–4912).
- Yin, G., Sheng, L., Liu, B., Yu, N., Wang, X., Shao, J., Loy, C.C. (2018). Zoom-net: Mining deep feature interactions for visual relationship recognition. *European conference on computer vision* (Vol. 11207, pp. 330–347).
- Yu, J., Chai, Y., Wang, Y., Hu, Y., Wu, Q. (2021). Cogtree: Cognition tree loss for unbiased scene graph generation. *International joint conference on artificial intelligence* (pp. 1274–1280).
- Zareian, A., Karaman, S., Chang, S. (2020). Bridging knowledge graphs to generate scene graphs. *European conference on computer vision* (Vol. 12368, pp. 606–623).
- Zellers, R., Yatskar, M., Thomson, S., Choi, Y. (2018). Neural motifs: Scene graph parsing with global context. *IEEE conference on computer vision and pattern recognition* (pp. 5831–5840).
- Zeng, P., Gao, L., Lyu, X., Jing, S., Song, J. (2021). Conceptual and syntactical cross-modal alignment with cross-level consistency for image-text matching. *Mm*.
- Zhan, Y., Yu, J., Yu, T., Tao, D. (2020). Multi-task compositional network for visual relationship detection. *International Journal of Computer Vision*, 128(8), 2146–2165.
- Zhang, H., Kyaw, Z., Chang, S., Chua, T. (2017). Visual translation embedding network for visual relation detection. *IEEE conference on computer vision and pattern recognition* (pp. 3107–3115).
- Zhang, M., Yang, Y., Zhang, H., Ji, Y., Shen, H.T., Chua, T. (2019). More is better: Precise and detailed image captioning using online positive recall and missing concepts mining. *IEEE Transactions on Image Processing*, 28(1), 32–44.
- Zhao, L., Lyu, X., Song, J., Gao, L. (2021). Guess-which? visual dialog with attentive memory network. *PR*.
- Zhao, S., Sharma, P., Levinboim, T., Soricut, R. (2019). Informative image captioning with external sources of information. (pp. 6485–6494).

Zheng, C., Gao, L., Lyu, X., Zeng, P., El-Saddik, A., Shen, H.T. (2023). Dual-branch hybrid learning network for unbiased scene graph generation.

Zheng, C., Lyu, X., Gao, L., Dai, B., Song, J. (2023). Prototype-based embedding network for scene graph generation. *CVPR*.

Zheng, C., Lyu, X., Guo, Y., Zeng, P., Song, J., Gao, L. (2022). Learning to generate scene graph from head to tail. *Icme*.